Sensors and Actuators B xxx (2009) xxx–xxx

Contents lists available at ScienceDirect

Sensors and Actuators B: Chemical

journal homepage: www.elsevier.com/locate/snb

Selective hydrogen gas nanosensor using individual ZnO nanowire with fast response at room temperature

O. Lupan[a,b,*], V.V. Ursaki[c], G. Chai[a], L. Chow[a,d], G.A. Emelchenko[e,f], I.M. Tiginyanu[g], A.N. Gruzintsev[f], A.N. Redkin[f]

[a] Department of Physics, University of Central Florida, PO Box 162385 Orlando, FL 32816-2385, USA
[b] Department of Microelectronics and Semiconductor Devices, Technical University of Moldova, 168 Stefan cel Mare Blvd., MD-2004, Chisinau, Republic of Moldova
[c] Institute of Applied Physics of the Academy of Sciences of Moldova, MD-2028, Chisinau, and National Center for Materials Study and Testing, Technical University of Moldova, MD-2004, Chisinau, Republic of Moldova
[d] Advanced Materials Processing and Analysis Center, and Department of Mechanical, Materials, and Aerospace Engineering, University of Central Florida, PO Box 162385 Orlando, FL 32816-2455, USA
[e] Institute of Solid State Physics, Russian Academy of Science, 142432 Chernogolovka, Moscow District, Russia
[f] Institute of Microelectronics Technology and High Purity Materials, Russian Academy of Sciences, 142432, Chernogolovka, Moscow District, Russia
[g] Laboratory of Nanotechnology, Institute of Electronic Engineering and Industrial Technologies, Academy of Sciences of Moldova, MD-2028, Chisinau, Moldova and National Center for Materials Study and Testing, Technical University of Moldova, MD-2004, Chisinau, Republic of Moldova

ARTICLE INFO

Article history:
Received 7 July 2009
Received in revised form 6 September 2009
Accepted 10 October 2009
Available online xxx

PACS:
81.05.Dz II–VI semiconductors
81.07.Bc Nanocrystalline materials

Keywords:
ZnO nanowire
Sensor
Hydrogen
Focused ion beam
Nanosensor

ABSTRACT

In this work, we report on a single ZnO nanowire-based nanoscale sensor fabricated using focused ion beam (FIB/SEM) instrument. We studied the diameter dependence of the gas response and selectivity of ZnO nanowires (NWs) synthesized by chemical vapor phase growth method. The photoluminescence (PL) measurements were used to determine the deep levels related to defects which are presented in the ZnO nanomaterial as well as to evaluate the effect of thermal treatment in H_2 atmosphere on the emission from ZnO nanowires. We show that sample annealed in hydrogen leads to passivation of recombination centers thus modifying the NWs properties.

We studied the gas response and selectivity of these ZnO nanowires to H_2, NH_3, *i*-Butane, CH_4 gases at room temperature. Our results indicated that zinc oxide NWs hold a high promise for nanoscale sensor applications due to its capability to operate at room-temperature and its ability to tune the gas response and selectivity by the defect concentration and the diameter of ZnO nanowire. A method is proposed to reduce the nanosensor's recovery time through the irradiation with an ultraviolet radiation pulse. The sensing mechanisms of ZnO nanowires will be discussed.

1. Introduction

The development of highly sensitive, selective, reliable, and compact sensing devices to detect flammable, toxic chemical and biological agents is of major importance. Over the last decades, bulk and thin film metal oxides have been widely studied and used for sensing gas species such as CO, CO_2, CH_4, C_2H_5OH, C_3H_8, H_2, H_2S, NH_3, NO, NO_2, O_2, O_3, SO_2, acetone, humidity, etc. [1–12]. The gas response to different gases is related to a great extent to the surface state and morphology of the material. However, some critical limitations are difficult to overcome with the sensors with micrometer dimension. In such materials, limited surface-to-volume ratio determines a limited gas response to low concentration of tested gases and requires operation at elevated temperatures to reach a desired gas response. In order to overcome these limitations different types of nanostructured materials and approaches have been investigated for their gas response, selectivity and possible application in sensors with better characteristics [12–18]. Particularly, nanorods/nanowires with their superior characteristics have caught the attention of researchers and have been investigated as sensor material by different groups [12,13,15,16,19–24]. The novel concepts for applications of these nanoscale materials in sensors and actuators are based on a generally strong coupling between electronic, chemical, optical and mechanical properties. Change of any one of these properties will affect others as well, a feature which is widely used in sensor applications. In addition, reproducibility

* Corresponding author at: Department of Physics, University of Central Florida, PO Box 162385 Orlando, FL 32816-2385, USA. Tel.: +1 407 823 2333; fax: +1 407 823 5112.
E-mail addresses: lupan@physics.ucf.edu, lupanoleg@yahoo.com (O. Lupan), chow@mail.ucf.edu (L. Chow).

0925-4005/$ – see front matter © 2009 Elsevier B.V. All rights reserved.
doi:10.1016/j.snb.2009.10.038

and long-term stability of sensor properties are important from the practical point of view.

However, several issues have to be resolved before applications of nanowires/nanorods can flourish, such as (a) the ability to handle individual nanowire, (b) the slow time constant for adsorption/desorption processes, and (c) the room temperature operation of the device. Recently, experimental investigations demonstrated evident changes in the electronic transport due to gas adsorption [9,10,24,25], which determine response/recovery time constants of the sensors. At the same time, the development of a recovery process which will allow cycled operation for multiple uses and satisfying long-term stability requirements for sensors is important. In this context, it is necessary to obtain more evidence of the correlation between aspect ratio, defects in nanowire (PL intensity ratio $\{I_{UV}/I_{DL}\}$) and its gas response as well as necessity/limits in operation at elevated temperatures or applications of thermal pulses during/between sensing cycles, etc. This means that adsorption and desorption of the gas molecules have to be controlled in order to design a fast response/recovery sensor. Different approaches/techniques of engineering were reported for solving this problem, such as the use of metal catalyst nanoparticle or chemical functional groups for surface functionalization, plasma treatment to increase resistivity or high temperature cycles, etc. [12–14,19,20–26]. According to another approach, Zhang et al. [21] have prepared NO_2 sensors based on In_2O_3 nanowires and the device recovery was realized by desorbing NO_2 molecules with ultraviolet (UV) light illumination. Peng et al. [22] observed that the gas response of nanorods to 110 ppm formaldehyde with UV light irradiation was about 120 times higher than that without UV light irradiation. One of the most common approaches is based on the high activation energy of reaction with gas molecules, thus respective high temperature is applied for the gas sensor to get higher response [12–14]. However, high temperature processes can be restrictive/forbidden for gas sensor applications in explosive environments, like hydrogen. Also, in order to develop high performance sensors (especially hydrogen sensor) based on ZnO nanowires it is preferred to avoid high temperature operation or uses of the heater to desorb foreign species/molecules from the surface in H_2 atmosphere for faster recovering process at elevated temperatures. This is motivated by the reduction of Zn from ZnO (which can make NW to disappear) and by the fact that recently in ZnO nanowire-based sensors a trend was found between gas sensitivity and defects in the nanomaterial [26,27]. It has been demonstrated that annealing in H_2, even at 400 °C, significantly reduces the green/red GRL emission, due to the passivation effect on the point defects or impurities, since the hydrogen atoms can easily diffuse into the lattice and form strong bonds with various lattice positions [27,28]. The gas sensitivity of defect-controlled gas sensors showed the same trends and gas sensitivity being linearly proportional to the defect density [26,27]. Considering all these aspects it is preferred to avoid long-term operation at high temperature or even short high temperature thermal pulses to desorb molecules from the ZnO surface, which may produce irreversible effects on nanowires properties. This will have direct and evident effects on long-term stability, which is the ability of the sensor to maintain its properties even when operated continuously for long duration in hostile medium. In this context, it is necessarily to mention that hydrogen is considered “the common fuel of the future” [15,16,29]. The goal of this work is to develop a room temperature hydrogen sensor based on a single ZnO nanowire.

In this work, we report on a single ZnO nanowire sensor fabricated using focused ion beam instrument. We present several proposals to improve room temperature sensor characteristics of a single ZnO nanowire to H_2 gas. The room temperature gas response and selectivity of diameter-selected ZnO nanowires are presented. The impact of a pulse of UV irradiation on gas sensing transient characteristics of a single ZnO nanowire is reported.

2. Experimental details

ZnO nanowires were grown by chemical vapor deposition (CVD) with a base pressure of 5 torr using high-purity (99.999%) Zn metal and an O_2/Ar flux as source chemicals. The preparation of the ZnO nanowires has been described in detail elsewhere [30–32]. The growth time was 30 min with the evaporation temperature of 670 °C (first zone), and the growth temperature of 650 °C (second zone). The synthesis was performed in a flowing type two-zone quartz reactor. In the first zone, zinc evaporated and in the second zone zinc vapors interacted with oxygen. The Si substrates were placed in the second zone. The oxygen–argon mixture was introduced into reactor at a flow rate of 1 l/h and the zinc consumption was about 20–28 g/h. The synthesis of ZnO nanowires takes place at approximately 30-fold excess of zinc vapors with respect to oxygen based on a molar ratio.

The morphologies and chemical composition microanalysis of zinc oxide samples were studied using a VEGA TESCAN TS 5130MM scanning electron microscope (SEM) equipped with an Oxford Instruments INCA energy dispersive X-ray (EDX) system. The EDX analysis of the ZnO nanowires indicated a stoichiometric ZnO composition (within a precision of 1 at%).

The continuous wave (cw) photoluminescence (PL) was excited by the 351.1 nm line of an Ar^+ Spectra Physics laser and analyzed with a double spectrometer ensuring a spectral resolution better than 0.5 meV. The samples were mounted on the cold station of a LTS-22-C-330 optical cryogenic system. The room temperature Raman scattering was investigated with a MonoVista CRS Confocal Laser Raman System in the backscattering geometry under the excitation by a 532 nm DPSS laser.

Two rigid contacts were made with a single ZnO nanowire on the nano-sensor substrate template (glass with Cr/Au contacts as contact electrodes) by using FIB metal deposition function. The test gas sensing characteristics were investigated using a sensor structure connected to external electrode in FIB system. The measuring apparatus consists of a closed quartz chamber connected to a gas flow system. The concentration of test gases was measured using a pre-calibrated mass flow controller. Test gas and air were introduced to a gas mixer via a two-way valve using separate mass flow controllers. The test gases were allowed to flow through a pipe network with a diameter of 5 mm to the test chamber with a sensor holder, in which the nanosensor was placed. By monitoring the output voltage across the nanorod-based sensor, the resistance was measured in dry air and in a test gas. A computer with suitable LabView interface handled all controls and acquisition of data.

3. Results and discussions

Fig. 1(a) shows the scanning electron microscope image of the cross-section of the ZnO nanowire arrays grown on Si(1 0 0) substrate placed in deposition zone at the entrance of the reactor (ratio O/Zn > 1). Fig. 1(b) presents the top-view image of samples synthesized at the exit zone in the reactor (ratio O/Zn < 1). The ZnO nanowires (NWs) grown at the exit zone (Fig. 1(b)) are thinner (100 nm in diameter) as compared to those produced at the entrance zone (200 nm) (Fig. 1(a)). The ZnO nanowires are several microns in length. Apart from that, the ZnO nanowires synthesized at the entrance zone (Fig. 1(a)) are better aligned as compared to more randomly pointed wires produced at the exit zone (Fig. 1(b)).

As mentioned above, it is known that structural defects strongly influence the electrical parameters of the zinc oxide which are extremely important for the gas sensor applications. According to

Please cite this article in press as: O. Lupan, et al., Selective hydrogen gas nanosensor using individual ZnO nanowire with fast response at room temperature, Sens. Actuators B: Chem. (2009), doi:10.1016/j.snb.2009.10.038

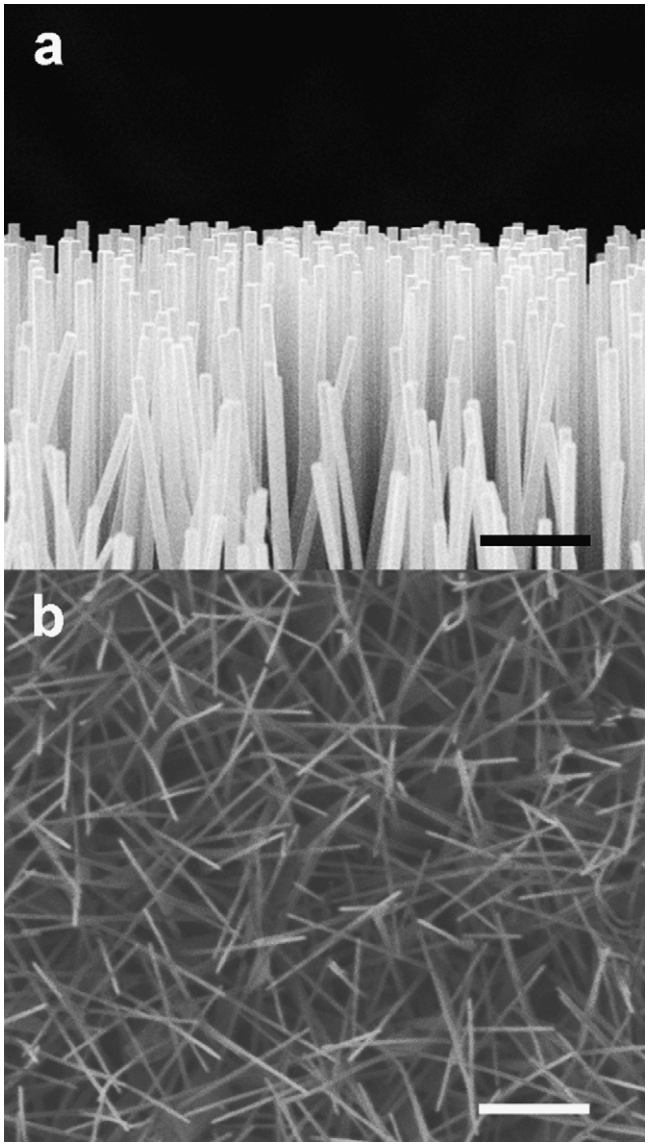

Fig. 1. (a) Scanning electron micrograph in cross-section of ZnO nanowires grown in deposition region at the entrance zone (ratio O/Zn > 1). (b) Top view scanning electron micrograph of ZnO nanowires grown at the exit zone (ratio O/Zn < 1). Scale bar is 2 μm.

previous predictions, the surface defects, such as oxygen vacancies, can dominate the electronic/chemical properties and adsorption behavior of metal oxide surfaces [33–35]. Deep levels (DL) are known to severely affect the optical and electrical properties of ZnO-based devices. It has been shown experimentally that ZnO material with a high density of oxygen vacancies has a high electrical conductivity [35]. Defects can influence substantially the sensitivity of gas sensors based on ZnO NWs [26,27].

Photoluminescence is a technique which can provide data related to DL, and the ratio I_{UV}/I_{DL} (the intensity of the ultraviolet to the visible deep level related luminescence) is a measure of defect states in ZnO nanomaterial. Fig. 2 displays the photoluminescence spectra of ZnO nanowires with diameter of 100 nm and 200 nm as curves 1 and 2, respectively. As previously reported, typical zinc oxide exhibits an ultraviolet (UV) emission (at about 380 nm at room temperature) due to near band-edge transitions [36]. The spectrum of the near band-edge emission is dominated by the excitonic luminescence, while the emission related to the donor–acceptor (DA) pair recombination is around two orders of magnitude less intensive (Fig. 2). The origin of the DA luminescence band has been previously investigated in detail [37–39].

The visible emission is a combination of a red and a green PL band. Usually, the red and the green luminescence is attributed to different structural defects such as oxygen vacancy (V_O), zinc vacancy (V_{Zn}) or a complex defect involving interstitial zinc (Zn_i) and interstitial oxygen (O_i) [35–44]. The low intensity of the visible emission as compared to the near band-edge one is an indication of a low concentration of defects. Considering recent reports, which demonstrated that the structural defects strongly influence the electrical parameters of the ZnO material [26,27,35], it is very important to study PL of ZnO NWs to be used in gas sensor structures.

Although both samples were synthesized in the same run, variations are observed in PL intensity (Fig. 2). The differences in spectra can be explained by different conditions of growth. The ZnO nanowires grown closer to the entrance of the tube furnace have a lower defect concentration because of higher O/Zn ratio and growth temperature, *i.e.* they are of a higher crystallinity. One can deduce from the analysis of Fig. 2(b) that the intensity of green (red) luminescence is a factor of 2 (3) higher in the nanowires with diameter of 100 nm as compared to the NWs with the diameter of 200 nm, while the intensity of the near band-edge luminescence is an order of magnitude lower. This means that the concentration of structural defects decreases with the increase in the diameter of the nanowire.

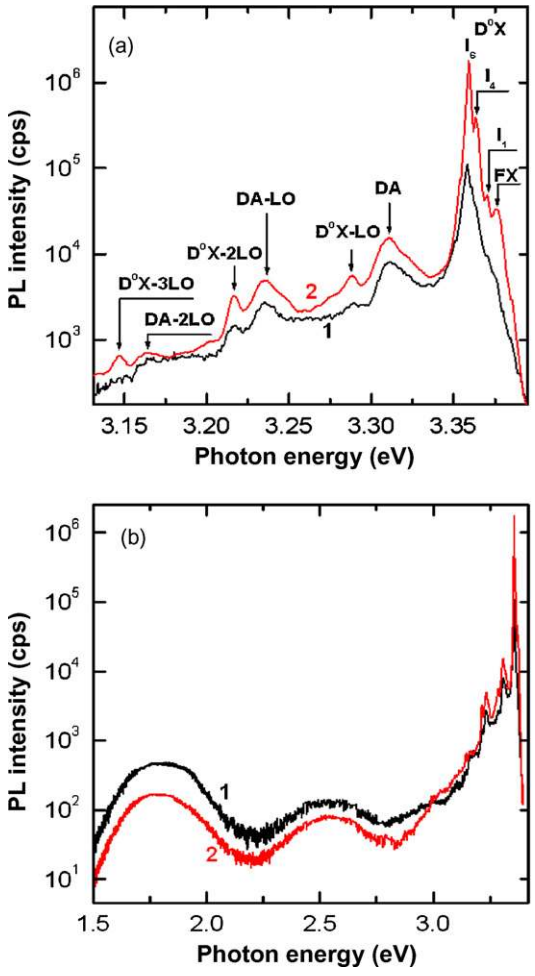

Fig. 2. (a) Emission spectra in ultraviolet UV region of the ZnO nanowires grown by CVD. (b) PL spectra in UV–vis region. Curve 1 corresponds to nanowires with diameter of 100 nm and curve 2 is for wires with diameter of 200 nm.

Please cite this article in press as: O. Lupan, et al., Selective hydrogen gas nanosensor using individual ZnO nanowire with fast response at room temperature, Sens. Actuators B: Chem. (2009), doi:10.1016/j.snb.2009.10.038

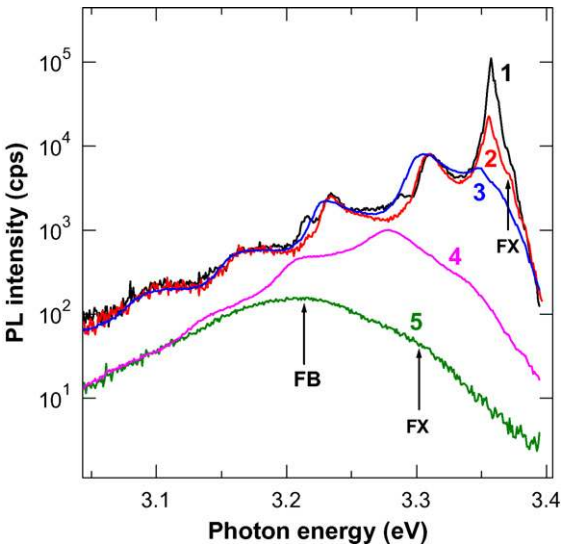

Fig. 3. PL spectra of ZnO nanowires with diameter of 100 nm measured at different temperatures: 1–20 K; 2–50 K; 3–100 K; 4–200 K; 5–300 K.

Apart from the analysis of the visible emission, the increase in the quality of nanowires with increasing diameter is suggested by the following observations: (i) the overall PL intensity increase with increasing the diameter; (ii) the intensity of the neutral donor bound exciton luminescence relative to the DA luminescence also increases; (iii) different lines related to different donors are better resolved in the PL spectrum, therefore, the spectrum is dominated by I_1, I_4, and I_6 lines [45] of the neutral donor bound excitons D^0X; (iv) the emission related to the recombination of free excitons FX becomes clearly resolved in the PL spectrum.

The other PL bands observed in the spectra are associated with the phonon replica of the neutral donor bound excitons D^0X and donor acceptor pair recombination DA PL lines. The suggested origin of the PL bands is corroborated by the analysis of the temperature dependence of the PL spectra (Fig. 3).

As temperature increases, PL related to the D^0X excitons and its phonon replica is rapidly quenched. The rate of decrease of the PL associated with the recombination of free excitons is smaller than the one for D^0X transitions. This is due to the larger binding energy of free excitons. Therefore, the FX band is observable up to room temperature as a shoulder on the high energy wing of the PL spectrum. The position of the FX band shifts from 3.376 eV at 20 K to 3.30 eV at room temperature in accordance with the temperature dependence of the A-exciton energy. While the PL band positioned at 3.21 eV at room temperature is assigned here to a free-to-bound FB-transition, a similar PL band was previously suggested to be related to donor–acceptor pair (DAP) transitions [46]. However, this emission is more likely related to the recombination of free electrons with holes bound at an acceptor, due to the temperature induced ionization of donor impurities involved in DAP transitions at low temperatures. The photon energy separation between the FB and FX bands is about 90 meV. By adding the binding energy of free excitons (60 meV) to this value one can estimate the activation energy of the defects responsible for the FB PL band to be on the order of 150 meV.

We studied the effects of thermal treatment at relatively low temperature (400 °C) in H_2 ambient on the optical properties of ZnO nanowires. PL was measured to evaluate the impact of thermal annealing in H_2 atmosphere on the emission from ZnO nanowires, especially in the deep levels (DLs) region. This was performed taking into account that nanowires are designed for H_2 gas nanoscale sensors, as well as considering the long-term stability of sensors when operating in hydrogen environment. This study is very important, since hydrogen is known to act as a donor in ZnO [47–49], and it can influence the properties of zinc oxide material.

Our investigations demonstrate that the concentration of defects responsible for visible emission DLs from ZnO nanowires was reduced by annealing at 400 °C in hydrogen atmosphere. As one can see from Fig. 4, the intensity of the green emission is reduced by a factor of 1.5 at low temperature, and by a factor of 2 at room temperature, while the intensity of the red emission is reduced by a factor of 3 at both temperatures after annealing in hydrogen. We observed that hydrogen annealing leads to passivation of recombination centers and to modification of NWs properties. Here we found passivation of DL donors and acceptors via electron transfer between defects and hydrogen, for instance:

$$V_O^{\bullet} + H_i^x \rightarrow V_O^x + H_i^{\bullet} \quad (1)$$

It was demonstrated theoretically that the hydrogen forms a shallow donor state in ZnO [48]. Therefore, charge compensation occurs when hydrogen co-exists with defects. The observed hydrogenation effects for CVD nanowires lead to passivation of DL states and influence their properties. These effects must be taken into account when analyzing long-term stability of nanosensors made on a single ZnO nanowire. Thus, PL investigations of nanomaterial properties suggest its suitability for the development of stable room temperature H_2 sensor from a single ZnO nanowire.

Also, it is necessary to mention that thermal annealing at temperatures higher than 400 °C in hydrogen atmosphere leads to Zn reduction in ZnO. This will lead to evaporation of zinc oxide nanowires, which confirms the necessity to develop a room temperature ZnO NW H_2 sensor.

The vibrational properties of ZnO nanowires are important in order to understand transport properties and phonon interaction with the free carriers, which determine device performance. Raman measurements provide information about the material quality [50–52]. We used Raman spectroscopy to investigate the crystalline quality of nanowires, in parallel with PL spectroscopy used to ana-

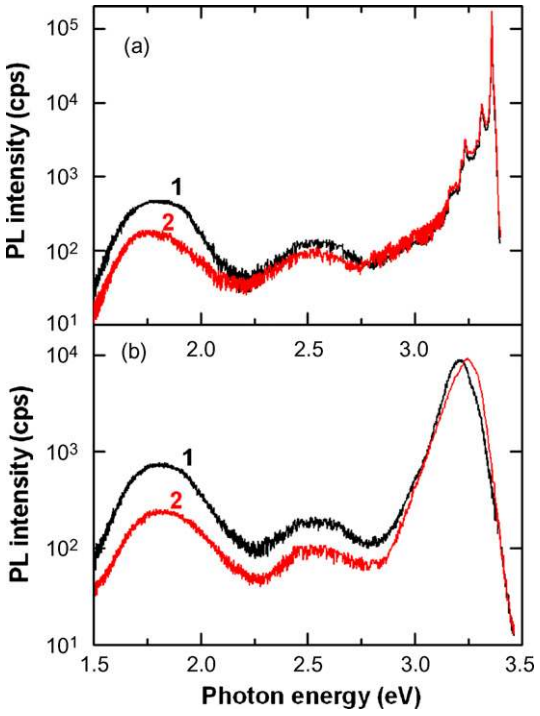

Fig. 4. PL spectra of ZnO nanowires with diameter of 100 nm. Curve 1 corresponds to as-grown sample, and curve 2 is for the sample annealed in hydrogen atmosphere at 400 °C. The spectra are measured at 10 K (a) and 300 K (b).

Please cite this article in press as: O. Lupan, et al., Selective hydrogen gas nanosensor using individual ZnO nanowire with fast response at room temperature, Sens. Actuators B: Chem. (2009), doi:10.1016/j.snb.2009.10.038

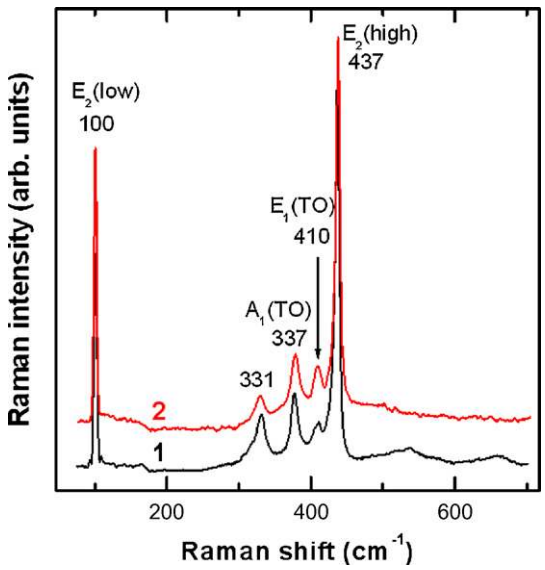

Fig. 5. Room-temperature micro-Raman spectrum of ZnO nanowires with diameter of 100 nm (curve1), and 200 nm (curve2).

lyze radiative defects, deep levels and their relation to gas-sensing properties of nanowires. Fig. 5 shows the room-temperature micro-Raman spectrum (RS) of the ZnO NWs grown on a Si substrate. Curve 1 in Fig. 5 illustrates the Raman spectrum of the produced ZnO nanowires with diameter of 100 nm, while curve 2 is for sample with diameter of 200 nm.

This Raman spectrum demonstrates the high quality of the wurtzite crystal structure of our ZnO nanowires. Wurtzite ZnO belongs to the C_{6v} space group ($P6_3mc$). According to group theory, the corresponding zone centre optical phonons are of the following symmetry modes [53]:

$$\Gamma_{opt} = A_1 + 2B_1 + E_1 + 2E_2 \quad (2)$$

The $A_1 + E_1 + 2E_2$ modes are Raman active, while $2B_1$ phonons are silent. The low-frequency E_2 mode is predominantly associated with the non-polar vibration of the heavier Zn sublattice, while the high frequency E_2 mode involves predominantly the displacements of lighter oxygen atoms. The A_1 and E_1 modes are split into longitudinal optical (LO) and transverse optical (TO) components. Except for the LO modes, all Raman active phonon modes are clearly identified in the measured spectrum (Fig. 5).

The LO modes are not visible in the spectrum, likely due to the presence of a high free carrier concentration in the sample. The peak at 331 cm^{-1} is attributed to second order Raman processes involving acoustic phonons [54]. There are several indications of a good crystal quality of the produced nanowires: (i) the signal attributed to the two-phonon density of states (DOS) expected in the spectral range from 500 cm^{-1} to 700 cm^{-1} [55–57] is practically absent in the ZnO NW sample with a diameter of 200 nm; (ii) the peak corresponding to E_2 (high) mode has a line-width of about 6 cm^{-1}, while the line-width of the peak corresponding to E_2 (low) mode is about 3 cm^{-1}, which is comparable to values reported for high quality ZnO bulk crystals [58]; (iii) the position of the E_2 (high) peak corresponds to the phonon of a bulk ZnO crystal [58] indicating a strain-free state of the nanowire. The presence of a weak RS signal in the spectral range from 500 cm^{-1} to 700 cm^{-1} in ZnO NWs with 100 nm diameter as compared to its absence in NWs with 200 nm in diameter, confirms the increase of the optical quality of the nanowires with increasing their diameter as deduced also from the PL analysis.

Next, we describe the fabrication procedure of nanosensors by using individual ZnO NW released from an agglomeration of nanowires as-grown on initial substrate (Fig. 1). The ZnO nanowires can be released from the initial substrate by sonication in ethanol and then transferred to a SiO_2-coated Si substrate. We also used a direct contact technique to transfer nanowires by direct contact of the sample with a clean Si wafer and gently rub a few times. These procedures allow us to obtain a low density and uniformly distributed ZnO nanowires on the second substrate (Fig. 6(a)) for device fabrication (Fig. 6(b)). If one needs to lower the density of NWs, the above procedure can be repeated.

A scanning electron microscope image of the transferred ZnO nanowires is presented in Fig. 6. Focused ion beam (FIB/SEM) instrument was used to pattern metal electrodes contacting both ends of a single ZnO nanowire. The separation of the electrodes was about 5 μm. The fabricated device based on a single wire of 200 nm in diameter (insert of Fig. 6(b)) and 100 nm (insert of Fig. 6(c)) are presented.

Here we would like to draw attention to a few characteristics which allow very thin ZnO NW (50–100 nm in diameter) to be connected by using FIB/SEM instrument in comparison with other types of metal oxide nanowires. It is well known that FIB permits the localized maskless growth of metal or insulator materials. It works like local chemical vapor deposition (LCVD) and the occurring reactions are comparable to, for example, laser induced CVD and micro stereolithography [59]. However, maskless deposition cannot be achieved by conventional CVD methods, which is an advantage of FIB/SEM set-up. According to previous reports [59], the main differences are related to better resolution and lower deposition rate of FIB. Based on multiple previous works on TEM samples fabrications using FIB set-up, the depth of penetration of FIB-ions in material is about 2–20 nm after 2–3 h of continuous exposure [60–63]. In our work a single ZnO NW was exposed to FIB beam for less than 9 min. Also, it is necessary to mention about enhanced radiation hardness of ZnO NWs versus bulk ZnO layers according to previous works [64–66]. As reported previously, the room temperature bombardment by electrons [67], protons [68] and heavy ions [69] caused much less damages in ZnO than in other

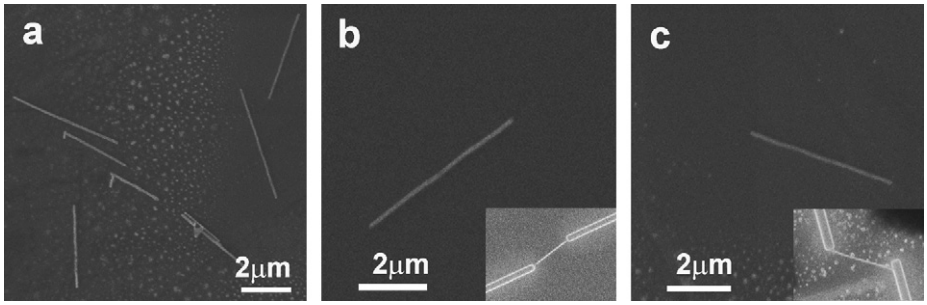

Fig. 6. Scanning electron micrographs of: (a) transferred ZnO nanowires (NWs) to intermediate substrate (Si with ZnO NWs on top); (b) transferred individual ZnO NW and insert shows a fabricated device based on a single ZnO nanowire of 200 nm in diameter; and (c) transferred ZnO NW and insert shows a fabricated device based on a single nanowire of 100 nm in diameter.

Please cite this article in press as: O. Lupan, et al., Selective hydrogen gas nanosensor using individual ZnO nanowire with fast response at room temperature, Sens. Actuators B: Chem. (2009), doi:10.1016/j.snb.2009.10.038

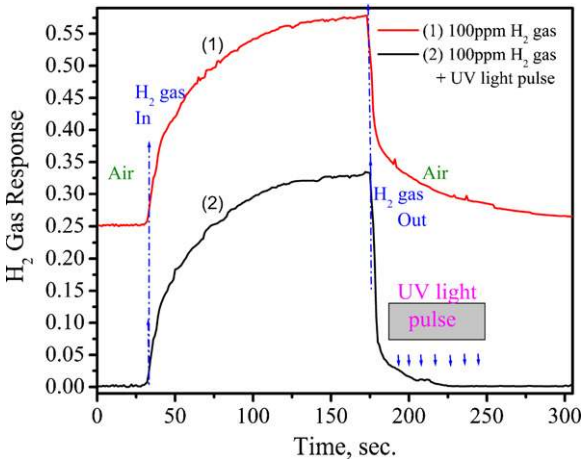

Fig. 7. Gas response curves of the 100 nm zinc oxide nanowire-based gas sensor under exposure to 100 ppm of H_2 gas at room temperature (22 °C). Curve (1) is displaced upward by 0.25 to avoid overlapping with curve (2).

semiconductors. This is a very important point here, since in our ion beam processing of nanostructured ZnO material, it is inevitable that ZnO nanostructures were exposed to ion beam.

It is to be noted that, according to Ref. [70], the FIB Ga ions started to affect the electric properties of ZnO providing that the dosage of the Ga ion beam exceeds 10^{15} cm^{-2}. During our FIB processing, the Ga ion beam can be very accurately positioned on the individual nanowire and the exposure time to Ga beam can be limited to just a few minutes. We estimated that our ZnO nanostructures were never exposed to Ga ion beam more than 10^{13} cm^{-2}, therefore the effect of FIB processing on our ZnO nanostrcutures has been minimized/insignificant [63]. This makes the ZnO nanodevices presented below feasible. However, few problems still need to be solved by using more modern equipment since, at this moment, we cannot completely rule out the accidental metal atom deposition on the ZnO NW during the FIB processing of electrode contact. However, we believe that the amount of the metal molecules accidentally deposited on ZnO NW is insignificant and has no particular influence on the response of these ZnO NW.

A linear behavior of the current-voltage curves (not shown) was observed, which is very important for the sensing properties because the gas response of a gas nanosensor can be maximized when the metal-semiconductor junction has a negligible resistance. For investigation of gas-sensing properties, a sensor was placed in a measuring apparatus consisting of a closed quartz chamber connected to a gas flow system. The concentration of test gases was measured using a pre-calibrated mass flow controller as described elsewhere [15,16,20].

The gas response was defined as the ratio:

$$S \approx \left| \frac{\Delta R}{R} \right|, \quad (3)$$

where $|\Delta R| = |R_{air} - R_{gas}|$ and R_{air} is the resistance of the sensor in dry air and R_{gas} is resistance in the test gas.

Fig. 7 shows the transient response of the 100 nm ZnO-nanowire gas sensor under exposure to 100 ppm of H_2 gas at room temperature. In Fig. 7 curve (1) is displaced upward by 0.25 in order to avoid overlapping with curve (2). An individual nanowire-based sensor displayed the highest gas response of about 34% to 100 ppm hydrogen gas at room temperature (22 °C). As seen from Fig. 7, both response and recovery times ($T = |t_{90\%} - t_{10\%}|$) were very fast, taking 64 s and 11 s for 90% of full response and recovery, respectively, at 100 ppm of H_2 gas.

As can be seen from Fig. 7 (curve 1, red color on-line) the resistance of the sensor after the exposure to hydrogen does not recover to the initial value, or even in 10% limit of the initial value. This is explained by the presence of adsorbed gas molecules, which still remain on the surface of ZnO nanowire. Usually, operation at elevated temperature is used in order to desorb the gas species from the surface of the sensor material [12–15,26,27].

However, our PL data (Figs. 5 and 6) suggest that it is desirable to avoid heating to desorb gas molecules, since it will change the properties of ZnO nanowires, particularly the defect states. As discussed above, the defects in nanomaterials influence the gas sensitivity of ZnO nanowire-based sensors [26,27]. Our unpublished data showed that the application of heating pulses to the sensor after H_2 gas was introduced in the test chamber leads to permanent changes of electrical properties of a single nanowire-based sensor and drifting of its sensing characteristics. It is evident that this shift is in contradiction with long-term stability requirements for sensors. Apart from that, heating is also undesirable for gas sensor applications in explosive environment, such as hydrogen.

We implement the UV irradiation procedure instead of heating to facilitate desorption of gas species on the surface and to improve the recovery time of the nanosensor. Fig. 7 (curve 2) demonstrates that the recovery time of the UV radiated sensor is much shorter than that of curve 1 (Fig. 7) and that of other types of gas sensors [71] reported before. The mechanism of reducing the recovery time of the UV radiated sensor has been described next.

Fig. 8 shows the performance of the zinc oxide nanowire sensor exposed to traces of 10 ppm H_2 gas at room temperature repeatedly.

As seen from Fig. 8, both response and recovery times ($T = |t_{90\%} - t_{10\%}|$) are much faster as compared to Fig. 7. The response and recovery time values at the level of 90% are about 3 s and 2 s, respectively, at 10 ppm of H_2. One can also observe by comparing Fig. 7(curve 2) and Fig. 8 that the gas response increases with increasing the concentration of H_2.

Therefore, we found experimentally that by applying the UV pulse one can facilitate desorption of gas molecules from the surface of ZnO nanowire (sensor resistance return to initial R_a value). We also mention that the gas nanosensor fabricated by this technique has similar or even higher gas response compared with those based on ZnO nanocrystals [72], ZnO nanorod [16] or ZnO branched rods [15], single tetrapod [20]. By comparison, the multiple ZnO nanorod-based sensor reported by Wang et al. [23] demonstrates a sensitivity of 4.2% at 500 ppm H_2 after 10 min exposure. Furthermore, the characteristics of a H_2 gas sensor based on ZnO multiple nanorods demonstrating 18% current change upon exposure to 10% H_2 in N_2 at 112 °C are considered to be satisfactory [18]. Wang et al.

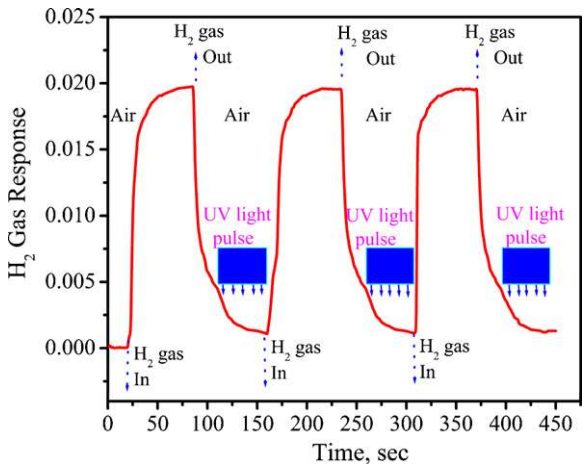

Fig. 8. Dependences of gas responses for 100 nm diameter ZnO NW-based sensor. The response curves of the individual nanowire-based sensor toward 10 ppm H_2 pulses. Before the test the nanowire was preconditioned in a constant dry air flow. An UV pulse is applied after H_2 gas is turned off.

Please cite this article in press as: O. Lupan, et al., Selective hydrogen gas nanosensor using individual ZnO nanowire with fast response at room temperature, Sens. Actuators B: Chem. (2009), doi:10.1016/j.snb.2009.10.038

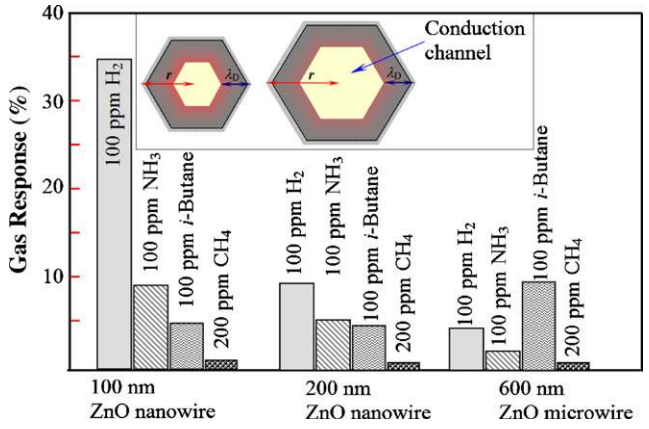

Fig. 9. Dependences of gas response for different diameter ZnO nanowire-based sensors. Insert shows cross-sectional view of ZnO NWs with different radii (r) and same Debye length (λ_D) and conduction channel, respectively.

[73] demonstrated sensitivity enhancement to 200 ppm H_2 gas of ZnO nanowires at higher temperatures (250 °C). By comparison, our single nanowire-based sensor (100 nm in diameter) shows similar characteristics upon 3 s exposure to H_2 gas at room temperature.

As mentioned above and reported previously [74], the gas species adsorbed by ZnO affect the charge carrier concentration and the resistance of zinc oxide. The larger surface-to-volume ratio of the single-crystalline nanowires offers potential to improve the gas response and selectivity of H_2 gas sensors. Our experimental results indicate that a ZnO single nanowire is an excellent material for H_2 sensors and should be further investigated in order to improve its characteristics at room temperature operation.

Gas selectivity has always been a major issue for the solid state gas sensors. Different approaches have been developed in the past to improve the selectivity of gas sensors, such as: (a) modulation of the operating temperature [14,75], (b) doping with metal impurities [17,76], (c) using impedance measurements [77], surface coating [78]. Fan and Lu [24] reported a solution for NO_2 and NH_3 room temperature sensors by introducing a concept of gate-refreshable ZnO nanowire field effect transistors. A transverse electric field induced by a back gate has been also proposed for selective gas sensing [79].

Fig. 9 demonstrates the dependence of the gas response on the diameter of ZnO NW-based sensors. The highest gas response (about 34%) was obtained from a sensor based on a single ZnO NW with 100 nm in diameter. In comparison, 200 nm NW showed a lower gas response to H_2 (less than 10%) at room temperature. A bigger diameter ZnO nanorod [16] demonstrated a gas response of about 4%. These observations demonstrate the importance of using thinner nanowires to design highly sensitive H_2 sensors which can operate at room temperature.

In order to test the selectivity of the gas sensor, the response to NH_3, *i*-Butane and CH_4 has been investigated and summarized in Fig. 9. We can see that the ZnO nanosensor's response to 100 ppm NH_3 and *i*-Butane or 200 ppm CH_4 is much lower in comparison with its gas response to H_2 gas. These data confirm the prospects of thin ZnO NWs as material for nanoscale sensors operating at room temperature. Although the gas response of thin ZnO NWs to *i*-Butane is low, we suggest that thicker ZnO NWs can be used to detect *i*-Butane-gas. These sensors may find applications in domestic or industrial environments.

4. Discussions related to possible sensing mechanism

Several factors determine the gas sensing mechanism of an individual ZnO nanowire. One of them is the value of the surface/volume ratio (aspect ratio) [80] of NW. Another one is the concentration and type of defects in ZnO NW [26,27] (which can be assessed by the (I_{UV}/I_{DL}) PL intensity ratio). The impact of these factors has been explained by physical effects occurring on the surface and in the volume of a ZnO nanowire [12,16,69,81]. It is known that metal oxide gas sensitivity depends on the interaction between the gas species and the adsorbed oxygen (O^{2-}, O^- and O^{2-}) ions on the surface or/and by interaction with defect states in the material.

Initially, when metal oxide nanowire is placed in air atmosphere the adsorbed oxygen (O_2^- and O^-) extracts electrons from the conduction band:

$$O_2(g) \leftrightarrow O_2(ad), \quad O_2(ad) + e^- \rightarrow O_2^-(ad), \quad \tfrac{1}{2}O_2 + e^- \rightarrow O^-(ad) \tag{4}$$

and an electron depletion region is formed which leads to the increase of the resistance of individual nanowire. Here it is necessarily to point out that the types of chemisorbed oxygen species depend strongly on temperature [74]. At lower temperatures, O_2^- is usually chemisorbed. However O^- and O^{2-} are commonly chemisorbed at higher temperatures, while O_2^- disappears rapidly [82]. Therefore, at room temperature a higher concentration of O_2^- ions on the surface of ZnO nanowire will allow a more effective interaction between H_2 and O_2^- ions and a higher sensitivity value. The oxygen chemisorption can be described by the following [74]:

$$\frac{\beta}{2}O_2^{Gas} + \alpha \cdot e^- + S \Leftrightarrow O_{\beta S}^{-\alpha} \tag{5}$$

where the oxygen molecule in atmosphere is O_2^{Gas}, e^- is an electron which can reach the surface, S is an unoccupied chemisorptions site for oxygen-surface oxygen vacancies and other surface defects. $O_{\beta S}^{-\alpha}$ is a chemisorbed oxygen species with $\alpha = 1, 2$ for single, doubly ionized form; $\beta = 1, 2$ for atomic, molecular forms, respectively.

The exchange of electrons between the bulk of ZnO NW and the surface states takes place within a surface layer (see insert in Fig. 9). The thickness of the surface layer is of the order of the Debye length/radius λ_D:

$$\lambda_D = \left(\frac{k\varepsilon_0 k_B T}{e^2 N_0}\right)^{1/2} \tag{6}$$

where N_0 is the density where the potential is zero, k_B is the Boltzmann constant and T is the absolute temperature in Kelvin, k is the relative static electric permittivity of the medium, ε_0 is the electric constant or is the permittivity of the free space and e is the elementary charge. This exchange will contribute to the decrease of the net carrier density in the nanowire conductance channel. Also this will lead to band bending near the surface for conduction and valence bands. The electrical conductance of ZnO nanowires can be expressed as dependent [24] upon the charge carriers' concentration:

$$G = \frac{1}{R} = \frac{\pi r^2}{\rho l} = \frac{n_0 |e| \mu \pi r^2}{l} \tag{7}$$

where R is electrical resistance, n_0 is the initial/nominal charge carriers concentration, e is the electron charge, μ is the mobility of electrons and r, l are the radius and length of the nanowire channel, respectively. Therefore, the change in electrical conductance of the nanowire exposed to gas atmosphere (Figs. 7 and 8) is determined by the change in electrical charge carriers' concentration Δn [83]:

$$\Delta G = \frac{(\Delta n_0 |e| \mu \pi r^2)}{l} \tag{8}$$

The gas sensitivity is given by [24,84]

$$\frac{\Delta G}{G} = \frac{\Delta n_s}{n_0} \tag{9}$$

Please cite this article in press as: O. Lupan, et al., Selective hydrogen gas nanosensor using individual ZnO nanowire with fast response at room temperature, Sens. Actuators B: Chem. (2009), doi:10.1016/j.snb.2009.10.038

According to this expression, higher gas sensitivity could be obtained by a larger modulation in the depletion region of ZnO nanowire. The width of the depletion region is inversely proportional to the square root of the free charge carrier concentration. When the radius of ZnO nanowire is in the order of or less than Debye length/radius, the conductive channel is reduced substantially (this is the case of thinner ZnO NW (see insert in Fig. 9)). The modulation of the depletion region width can also be produced by the control of electron density in ZnO nanowire, *i.e.* by means of surface defects.

The gas response of the resistive sensors in ambient medium may be given by the following equation:

$$S = \frac{G_g - G_a}{G_g} \cdot 100\% = \frac{4}{D}(\lambda_{D(a)} - \lambda_{D(g)}) \cdot 100\% = \frac{4}{D}\left(\left(\frac{k\varepsilon_0 k_B T}{e^2 N_0}\right)^{1/2} - \left(\frac{k\varepsilon_0 k_B T}{e^2 N_0}\right)^{1/2}\right) \cdot 100\% \quad (10)$$

or by following [85]:

$$S = \frac{G_g - G_a}{G_g} = \frac{4}{D}(\lambda_{D(a)} - \lambda_{D(g)}) = \frac{4}{D}\left(\frac{\varepsilon\varepsilon_0}{en_0}\right)^{1/2}(V_{Sa}^{1/2} - V_{Sg}^{1/2}) \quad (11)$$

where G_g and G_a are the conductance of ZnO nanowires in H_2 gas and in air ambient, respectively, n_0 is carrier concentration in air. V_{Sa} and V_{Sg} are the adsorbance-induced band bending in air and in H_2 gas, respectively. According to the last equation, enhancement of H_2 gas sensitivity can be realized by controlling the geometric factor ($4/D$), electronic characteristics ($\varepsilon\varepsilon_0/en_0$), and adsorption induced band bending ($V_{Sa}^{1/2} - V_{Sg}^{1/2}$) due to adsorption on ZnO nanowire surface. This can be done by doping, which is not our case, or by using modulation of operation temperature which is not desirable for H_2 sensors on single ZnO nanowire as discussed above. Another way is to make use of geometric parameters, which was realized in our experiments. By using different diameter NWs, sensors with different gas response characteristics were produced (Fig. 9).

Furthermore, when a nanosensor is exposed to hydrogen atmosphere the adsorption–desorption sensing mechanism can be explained on the basis of reversible gas chemisorptions on surface of the ZnO nanowire. A reversible variation in the electrical resistance is produced by the exchange of charges between the hydrogen and the ZnO surface which leads to the variation of the depletion depth. The electrons will be released to the conduction band and the current through nanowire will increase as a result of the following reactions:

$$H_2 + \tfrac{1}{2}O_2^-(ad) \rightarrow H_2O + e^- \quad (12)$$

$$H_2 + O^-(ad) \rightarrow H_2O + e^- \quad (13)$$

The hydrogen molecules will react with adsorbed oxygen ions on the surface of nanowire and will produce H_2O molecules, while the released electrons will contribute to the current increase through the nanowire. This will also reduce the width of the depletion region. The reaction is exothermic (1.8 kcal mol^{-1}) [86] and the molecular water desorbs quickly from the surface.

A higher concentration of O_2^- ions on the surface of ZnO nanowire will allow a more effective interaction between H_2 and O_2^- ions and a higher gas response value will be realized. We suggest that the higher gas response of our single nanowire gas sensor as compared to thin film sensors is mainly due to a larger surface-to-volume ratio and a more effective modulation of the surface depletion region in individual ZnO nanowire. Nevertheless, not all gas species are desorbed rapidly from the NW surface which compromises the response time of sensor. As mentioned in the experimental section of the paper, we propose to overcome this drawback through the application of UV radiation pulses instead of thermal agents. The mechanisms of improving the dynamic characteristics of the gas sensor by using UV pulses are explained as follows.

After the sensor is illuminated by UV light, the electron-hole ($e^- - h^+$) pairs are photogenerated ($h\nu \rightarrow e^- + h^+$). The electron-hole pairs are separated in the surface depletion charge region and the holes (h^+) diffusing/migrate to the surface to discharge the adsorbed gas species and to decrease the thickness of the depletion layer near the surface [87]:

$$h^+ + O_2^-(ad) \rightarrow O_2, \quad h^+ + O^-(ad) \rightarrow \tfrac{1}{2}O_2 \quad (14)$$

After trapping holes, the oxygen/gas species are photo-desorbed from the surface which results in reducing the depletion region. The unpaired electrons contribute to the decrease of the resistivity of ZnO nanowire. The entire process is dependent on the ambient atmosphere. The pulse of UV light applied to the sensor causes desorption of oxygen, gas ions and water molecules from the sensor surface, therefore producing clean ZnO nanowire surface [88,89]. This stimulates returning of ZnO nanowire sensor resistance to the initial R_a value by changing conduction channel of the single ZnO NW (see insert in Fig. 9). In this way a pulse of UV light facilitates the adsorbed gas to be easily desorbed and swept away from the surface of ZnO [22]. These findings brings us to the idea of the exploration of the effect of the UV light irradiation between pulses of lower concentrations of H_2 gas tests.

As discussed above, another component of gas sensitivity is related to defects, especially oxygen vacancies can act as adsorption sites for gas species. According to recent reports [26,27] surface defects such as oxygen vacancies can influence the electronic/chemical properties, adsorption behavior of metal oxides surfaces, and reversibility of sensor characteristics. The presence of oxygen vacancies in our samples is indicated by V_O-related luminescence emission at 490 nm (2.53 eV) [90]. The interaction of hydrogen molecule with surface defects is modeled as follows:

$$H_2 + \dot{O}_i \rightarrow H_2O + O_O^x + e' \qquad H_2 + \dot{V}_O + e' \rightarrow H_2O + O_O^x \quad (15)$$

where O_O^x is neutral oxygen in oxygen site, $\dot{V}_O$ is a positive charged oxygen vacancy, e' is negatively charged electron according to the Kröger-Vink notation [91]. According to previous reports [92] gas molecules can bind more tightly with oxygen vacancies, thus attracting more charge from zinc oxide surface compared with defect-free ZnO surface, which is in good agreement with the close relationship between the concentration of oxygen-related defects and H_2 sensitivity of ZnO gas sensor. Our experimental results corroborate the correlation between surface defects and gas-sensing property of a ZnO gas sensor.

Here we have to mention that the adsorption of hydrogen species on the ZnO surface has been in the focus of researchers for more than 40 years [93,94]. It is of great importance to understand the interaction of hydrogen with ZnO surfaces. This will enable the design of ZnO-based hydrogen sensors, especially by using nanowires as potential candidates for nanoscale devices. However, these processes are complicated by various types of hydrogen adsorption on ZnO, which are very sensitive to experimental conditions [93].

According to previous reports [93–95] chemisorbed hydrogen on ZnO surface is more often observed in experiments. It consists of dissociative and heterolytic chemisorption of H_2 on both surface Zn and O sites. The associate reaction is rapid and reversible at room temperature. However, further research is needed to clarify the sensing mechanism.

Conclusions on sensing mechanism:

(a) A smaller diameter of ZnO NW means that more atoms are surface atoms that will participate in surface reactions.

Please cite this article in press as: O. Lupan, et al., Selective hydrogen gas nanosensor using individual ZnO nanowire with fast response at room temperature, Sens. Actuators B: Chem. (2009), doi:10.1016/j.snb.2009.10.038

(b) A smaller diameter of ZnO NW means that the Debye length λ_D (a measure of the field penetration into the bulk) is comparable to the radius, which causes their electronic properties to be more influenced by adsorption–desorption processes at the surface.
(c) The response and recovery times of ZnO NW sensor are determined by the adsorption–desorption kinetics that depends on the operation temperature [26,27]. The increased electron and hole diffusion rate to the surface of the nanodevice allows the analyte to be rapidly photo-desorbed from the surface (a few seconds) even at room temperature under UV light pulse.
(d) ZnO nanowires grown by CVD exhibit stoichiometric composition and are characterized by a higher level of crystallinity than the multigranular oxides currently used in sensors. This should potentially reduce the instability associated with percolation or hopping conduction.

These results indicate that the surface depletion has a significant influence on the electronic transport behavior of ZnO nanowires since the depletion width can be comparable to the nanowire diameter. This explains why the operation mode of ZnO nanowire devices can be controlled by the modulation of surface states through surface morphology engineering and size control.

5. Conclusions

The nanoscale sensor based on a single ZnO nanowire (100 nm in diameter) was fabricated by using focused ion beam (FIB/SEM) instrument. The diameter dependence of the gas response and selectivity of a single ZnO nanowire (NW) synthesized by chemical vapor phase growth method was studied. It was shown that NWs annealing at 400 °C in hydrogen leads to passivation of recombination centers thus modifying the NWs properties and decreasing the gas responsivity.

It was demonstrated the dependence of the gas response on the diameter of ZnO NW-based sensors and the highest gas response (about 34%) was obtained from a sensor based on a single ZnO NW with 100 nm in diameter. For comparison, 200 nm NW shows a lower gas response to H_2 (less than 10%) at room temperature. It was found that the fabricated ZnO NW nanosensor response to 100 ppm NH_3 and *i*-Butane or 200 ppm CH_4 is much lower in comparison with the response to H_2 gas.

The gas response and selectivity of the ZnO nanowires to H_2, NH_3, *i*-Butane, CH_4 gases at room temperature demonstrate that a single NW holds a high promise for nanoscale sensor applications. This is supported by the capability to operate at room temperature and the possibility to tune the gas response and selectivity by the surface defect concentration and the diameter of ZnO nanowire.

The obtained dependences of the gas response for different diameter ZnO nanowire-based sensors are discussed considering cross-sectional view of ZnO NWs with different radii (r), same Debye length (λ_D) and conduction channel, respectively. Our experimental data confirm the prospects of thin ZnO NWs as active elements for nanoscale sensors operating at room temperature. The reduction of the nanosensor's recovery time through the irradiation with an ultraviolet radiation pulse was demonstrated. The sensing mechanisms of ZnO nanowires were elucidated.

Acknowledgements

L. Chow acknowledges partial financial support from Apollo Technologies, Inc. and Florida High Tech Corridor Program. Financial supports by the Russian Foundation for Basic Research (Project No 08-02-90103) and Supreme Council for Science and Technological Development of the Academy of Sciences of Moldova (Project 036/R) are gratefully acknowledged. Dr. Lupan acknowledges financial support for post-doctoral position in Professor Chow's group.

References

[1] A.M. Azad, S.A. Akbar, S.G. Mhaisalkar, L.D. Birkefeld, K.S. Goto, Solid-state gas sensors—a review, J. Electrochem. Soc. 139 (1992) 3690–3704.
[2] G. Eranna, B.C. Joshi, D.P. Runthala, R.P. Gupta, Oxide materials for development of integrated gas sensors—a comprehensive review, Cristal Rev. Solid State Mater. Sci. 29 (2004) 111–188.
[3] C. Wang, X. Chu, M. Wu, Detection of H_2S down to ppb levels at room temperature using sensors based on ZnO nanorods, Sens. Actuators B: Chem. 113 (2006) 320–323.
[4] B.S. Kang, S. Kim, F. Ren, K. Ip, Y.W. Heo, B.P. Gila, C.R. Abernathy, D.P. Norton, S.J. Pearton, Detection of CO using bulk ZnO Schottky rectifiers, Appl. Phys. A 80 (2005) 259–261.
[5] S. Jung, H. Yanagida, The characterization of a CuO/ZnO heterocontact-type gas sensor having selectivity for CO gas, Sens. Actuators B: Chem. 37 (1996) 55–60.
[6] Q. Wan, Q.H. Li, Y.J. Chen, T.H. Wang, X.L. He, J.P. Li, C.L. Lin, Fabrication and ethanol sensing characteristics of ZnO nanowire gas sensors, Appl. Phys. Lett. 84 (2004) 3654–3656.
[7] W. Park, J.S. Kim, G. Yi, M.H. Bae, H.-J. Lee, Fabrication and electrical characteristics of high-performance ZnO nanorod field-effect transistors, Appl. Phys. Lett. 85 (2004) 5052–5054.
[8] C. Yu, Q. Hao, S. Saha, L. Shi, X. Kong, Z.L. Wang, Integration of metal oxide nanobelts with microsystems for nerve agent detection, Appl. Phys. Lett. 86 (2005) 063101.
[9] C. Li, D. Zhang, X. Liu, S. Han, T. Tang, J. Han, C. Zhou, In_2O_3 nanowires as chemical sensors, Appl. Phys. Lett. 82 (2003) 1613–1615.
[10] J. Kong, N.R. Franklin, C. Zhou, M.G. Chapline, S. Peng, K. Cho, H. Dai, Nanotube molecular wires as chemical sensors, Science 287 (2000) 622–625.
[11] A. Kolmakov, Y. Zhang, G. Cheng, M. Moskovits, Detection of CO and O_2 using tin oxide nanowire sensors, Adv. Mater. 15 (2003) 997–1000.
[12] A. Kolmakov, M. Moskovits, Chemical sensing and catalysis by one-dimensional metal-oxide nanostructures, Annu. Rev. Mater. Res. 34 (2004) 151–180.
[13] Z.L. Wang, Zinc oxide nanostructures: growth, properties and applications, J. Phys.: Condensed Matter 16 (2004) R829–R858.
[14] S.T Shishiyanu, T.S. Shishiyanu, O.I. Lupan, Sensing characteristics of tin-doped ZnO thin films as NO_2 gas sensor, Sens. Actuators B: Chem. 107 (2005) 379–386.
[15] O. Lupan, G. Chai, L. Chow, Fabrication of ZnO nanorod-based hydrogen gas nanosensor, Microelectron. J. 38 (2007) 1211–1216.
[16] O. Lupan, G. Chai, L. Chow, Novel hydrogen gas sensor based on single ZnO nanorod, Microelectron. Eng. 85 (2008) 2220–2226.
[17] O. Lupan, L. Chow, S. Shishiyanu, E. Monaico, T. Shishiyanu, V. Şontea, B. Roldan Cuenya, A. Naitabdi, S. Park, A. Schulte, Nanostructured zinc oxide films synthesized by successive chemical solution deposition for gas sensor applications, Mater. Res. Bull. 44 (2009) 63–69.
[18] B.S. Kang, Y.W. Heo, L.C. Tien, D.P. Norton, F. Ren, B.P. Gila, S.J. Pearton, Hydrogen and ozone gas sensing using multiple ZnO nanorods, Appl. Phys. A 80 (2005) 1029–1032.
[19] L.C. Tien, P.W. Sadik, D.P. Norton, L.F. Voss, S.J. Pearton, H.T. Wang, B.S. Kang, F. Ren, J. Jun, J. Lin, Hydrogen sensing at room temperature with Pt-coated ZnO thin films and nanorods, Appl. Phys. Lett. 87 (2005) 222106–222108.
[20] O. Lupan, L. Chow, G. Chai, A single ZnO tetrapod-based sensor, Sens. Actuators B: Chem. 141 (2) (2009) 511–517.
[21] D. Zhang, Z. Liu, Ch. Li, T. Tang, X. Liu, S. Han, B. Lei, Ch. Zhou, Detection of NO_2 down to ppb levels using individual and multiple In_2O_3 nanowire devices, Nano Lett. 4 (10) (2004) 1919–1924.
[22] L. Peng, Q. Zhao, D. Wang, J. Zhai, P. Wang, S. Pang, T. Xie, Ultraviolet-assisted gas sensing: a potential formaldehyde detection approach at room temperature based on zinc oxide nanorods, Sens. Actuators B: Chem. 136 (2009) 80–85.
[23] H.T. Wang, B.S. Kang, F. Ren, L.C. Tien, P.W. Sadik, D.P. Norton, S.J. Pearton, Jenshan Lin, Hydrogen-selective sensing at room temperature with ZnO nanorods, Appl. Phys. Lett. 86 (2005) 243503–243505.
[24] Z.Y. Fan, J.G. Lu, Gate-refreshable nanowire chemical sensors, Appl. Phys. Lett. 86 (2005) 123510.
[25] E. Comini, G. Faglia, G. Sberveglieri, Z. Pan, Z.L. Wang, Stable and highly sensitive gas sensors based on semiconducting oxide nanobelts, Appl. Phys. Lett. 81 (2002) 1869–1871.
[26] L. Liao, H.B. Lu, J.C. Li, C. Liu, D.J. Fu, Y.L. Liu, The sensitivity of gas sensor based on single ZnO nanowire modulated by helium ion radiation, Appl. Phys. Lett. 91 (2007) 173110.
[27] M.-W. Ahn, K.-S. Park, J.-H. Heo, J.-G. Park, D.-W. Kim, K.J. Choi, J.-H. Lee, S.-H. Hong, Gas sensing properties of defect-controlled ZnO-nanowire gas sensor, Appl. Phys. Lett. 93 (2008) 263103.
[28] S.H. Jo, J.Y. Lao, Z.F. Ren, R.A. Farrer, T. Baldachini, J.T. Fourkas, Field-emission studies on thin films of zinc oxide nanowires, Appl. Phys. Lett. 83 (2003) 4821–4823.
[29] "Basic Research Needs to Assure a Secure Energy Future," A Report from the Basic Energy Sciences Advisory Committee (February 2003). available at http://www.sc.doe.gov/bes/besac/Basic_Research_Needs_To_Assure_A_Secure_Energy_Future_FEB2003.pdf.

Please cite this article in press as: O. Lupan, et al., Selective hydrogen gas nanosensor using individual ZnO nanowire with fast response at room temperature, Sens. Actuators B: Chem. (2009), doi:10.1016/j.snb.2009.10.038

[30] A.N. Redkin, Z.I. Makovei, A.N. Gruzintsev, S.V. Dubonos, E.E. Yakimov, Vapor phase synthesis of aligned ZnO nanorod arrays from elements, Inorg. Mater. 43 (2007) 253–257.
[31] O. Lupan, G.A. Emelchenko, V.V. Ursaki, G. Chai, A.N. Redkin, A.N. Gruzintsev, I.M. Tiginyanu, L. Chow, L.K. Ono, B. Roldan Cuenya, H. Heinrich, E.E. Yakimov, Synthesis and characterization of ZnO nanowires for nano-sensor applications, under Review.
[32] O. Lupan, G. Chai, L. Chow, G.A. Emelchenko, V.V. Ursaki, A.N. Gruzintsev, I.M. Tiginyanu, A.N. Redkin, H. Heinrich, Ultraviolet photoconductive sensor employing a single ZnO nanowire, in: E-MRS 2009 Spring Meeting, June 8–12, Strasbourg, France, 2009.
[33] E. Henrich, P.A. Cox, The Surface Science and Metal Oxides, Cambridge University Press, Cambridge, 1994.
[34] R. Schaub, E. Wahlstrom, A. Ronnaus, E. Laegsgaard, I. Stensgaard, F. Besenbacher, Oxygen-mediated diffusion of oxygen vacancies on the TiO_2(1 1 0) surface, Science 299 (2003) 377–379.
[35] P.C. Chang, Z. Fan, D. Wang, W.Y. Tseng, W.A. Chiou, J. Hong, J.G. Liu, ZnO nanowires synthesized by vapor trapping CVD method, Chem. Mater. 16 (2004) 5133–5137.
[36] Ü. Özgür, Y.I. Alivov, C. Liu, A. Teke, M.A. Reshchikov, S. Dogan, V. Avrutin, S.-J. Cho, H. Morkoc, A comprehensive review of ZnO materials and devices, J. Appl. Phys. 98 (2005) 041301.
[37] V.V. Ursaki, I.M. Tiginyanu, V.V. Zalamai, V.M. Masalov, E.N. Samarov, G.A. Emelcenko, F. Briones, Photoluminescence of ZnO layers grown on opals by chemical deposition from zinc nitrate solution, Semiconductor Sci. Technol. 19 (2004) 851–854.
[38] S.T. Shishiyanu, O.I. Lupan, E.V. Monaico, V.V. Ursaki, T.S. Shishiyanu, I.M. Tiginyanu, Photoluminescence of chemical bath deposited ZnO:Al films treated by rapid thermal annealing, Thin Solid Films 488 (2005) 15–19.
[39] V.V. Ursaki, O.I. Lupan, L. Chow, I.M. Tiginyanu, V.V. Zalamai, Rapid thermal annealing induced change of the mechanism of multiphonon resonant Raman scattering from ZnO nanorods, Solid State Commun. 143 (2007) 437–441.
[40] H.C. Ong, G.T. Du, The evolution of defect emissions in oxygen-deficient and -surplus ZnO thin films: the implication of different growth modes, J. Crystal Growth 265 (2004) 471–475.
[41] A.B. Djurisic, Y.H. Leung, K.H. Tam, Y.F. Hsu, L. Ding, W.K. Ge, Y.C. Zhong, K.S. Wong, W.K. Chan, H.L. Tam, K.W. Cheah, W.M. Kwok, D.L. Phillips, Defect emissions in ZnO nanostructures, Nanotechnology 18 (2007) 095702.
[42] X.Y. Kang, Z.L. Wang, Polar-surface dominated ZnO nanobelts and the electrostatic energy induced nanohelixes, nanosprings, and nanospirals, Appl. Phys. Lett. 84 (2004) 975–977.
[43] J.W. Hu, Y. Bando, Growth and optical properties of single-crystal tubular ZnO whiskers, Appl. Phys. Lett. 82 (2003) 1401–1403.
[44] D.C. Look, G.C. Farlow, P. Reunchan, S. Limpijumnong, S.B. Zhang, K. Nordlund, Native-defect donors in n-type ZnO, Phys. Rev. Lett. 95 (2005) 225502.
[45] B.K. Meyer, H. Alves, D.M. Hofmann, W. Kriegseis, D. Forster, F. Bertram, J. Christen, A. Hoffmann, M. Straßburg, M. Dworzak, U. Haboeck, A.V. Rodina, Bound exciton and donor–acceptor pair recombinations in ZnO, Phys. Status Solidi (b) 241 (2004) 231–260.
[46] S.-H. Park, C.-H. Choi, K.-B. Kim, S.-H. Kim, Influences of ZnO buffer layers on the quality of ZnO films synthesized by the metal-organic chemical vapor deposition process, J. Electron. Mater. 32 (2003) 1148–1154.
[47] D.G. Thomas, J.J. Lander, Hydrogen as a donor in zinc oxide, J. Chem. Phys. 25 (1956) 1136–1142.
[48] G. Chris, V. de Walle, Hydrogen as a cause of doping in zinc oxide, Phys. Rev. Lett. 85 (2000) 1012–1015.
[49] (a) K. Ip, M.E. Overberg, Y.W. Heo, D.P. Norton, S.J. Pearton, C.E. Stutz, S.O. Kucheyev, C. Jagadish, J.S. Williams, B. Luo, F. Ren, D.C. Look, J.M. Zavada, Hydrogen incorporation, diffusivity and evolution in bulk ZnO, Solid State Electron. 47 (2003) 2255–2259;
(b) W. Liu, B. Yao, Y. Li, B. Li, C. Zheng, B. Zhang, C. Shan, Z. Zhang, J. Zhang, D. Shen, Annealing temperature dependent electrical and optical properties of ZnO and MgZnO films in hydrogen ambient, Appl. Surf. Sci. 255 (2009) 6745.
[50] N. Hasuike, H. Fukumura, H. Harima, K. Kisoda, H. Matsui, H. Saeki, H. Tabata, Raman scattering studies on ZnO doped with Ga and N (codoping), and magnetic impurities, J. Phys.: Condensed Matter 16 (2004) S5807–s5810.
[51] W. Limmer, W. Ritter, R. Sauer, B. Mensching, C. Liu, B. Rauschenbach, Raman scattering in ion-implanted GaN, Appl. Phys. Lett. 72 (1998) 2589–2591.
[52] D. Pastor, R. Cuscó, L. Artús, G. González-Díaz, S. Fernández, E. Calleja, Effect of the implantation temperature on lattice damage of Be^+-implanted GaN, Semiconductor Sci. Technol. 20 (2005) 374–377.
[53] A. Kaschner, U. Haboeck, M. Strassburg, M. Strassburg, G. Kaczmarczyk, A. Hoffmann, C. Thomsen, A. Zeuner, H.R. Alves, D.M. Hofmann, B.K. Meyer, Nitrogen-related local vibrational modes in ZnO:N, Appl. Phys. Lett. 80 (2002) 1909–1911.
[54] M. Rajalakshmi, A.K. Arora, B.S. Bendre, S. Mahamuni, Optical phonon confinement in zinc oxide nanoparticles, J. Appl. Phys. 87 (2000) 2445–2448.
[55] F. Reuss, C. Kichner, Th. Gruber, R. Kling, S. Maschek, W. Limmer, A. Waag, P. Ziemann, Optical investigations on the annealing behavior of gallium- and nitrogen-implanted ZnO, J. Appl. Phys. 95 (2004) 3385–3390.
[56] J. Serrano, A.H. Romero, F.J. Manjon, R. Lauck, M. Cardona, A. Rubio, Pressure dependence of the lattice dynamics of ZnO: an ab initio approach, Phys. Rev. B 69 (2004) 094306.
[57] L. Chow, O. Lupan, H. Heinrich, G. Chai, Self-assembly of densely packed and aligned bilayer ZnO nanorod arrays, Appl. Phys. Lett. 94 (2009) 163105.
[58] J. Serrano, F.G. Manjon, A.H. Romero, F. Widulle, R. Lauck, M. Cardona, Dispersive phonon linewidths: the E_2 phonons of ZnO, Phys. Rev. Lett. 90 (2003) 055510.
[59] S. Reyntjens, R. Puers, A review of focused ion beam applications in microsystem technology, J. Micromech. Microeng. 11 (2001) 287–300.
[60] S. Dhara, A. Datta, C.T. Wu, Z.H. Lan, K.H. Chen, Y.L. Wang, L.C. Chen, C.W. Hsu, H.M. Lin, C.C. Chen, Enhanced dynamic annealing in Ga^+ ion-implanted GaN nanowires, Appl. Phys. Lett. 82 (2003) 451.
[61] A.J. Steckla, I. Chyr, Focused ion beam micromilling of GaN and related substrate materials (sapphire, SiC, and Si), J. Vac. Sci. Technol. B 17.2 (1999) 362–365.
[62] S. Rubanov, P.R. Munroe, FIB-induced damage in silicon, J. Microsc. 214 (Pt 3) (2004) 213–221.
[63] G. Chai, O. Lupan, L. Chow, Focused ion beam fabrication of carbon nanotube and ZnO nanodevices, Nanofabrication Using Focused Ion and Electron Beams: Principles and Applications, in: P. Russell, I. Utke, S. Moshkalev (Eds.), 2010.
[64] A. Burlacu, V.V. Ursaki, V.A. Skuratov, D. Lincot, T. Pauporté, H. Elbelghiti, E. Rusu, I.M. Tiginyanu, The impact of morphology upon the radiation hardness of ZnO layer, Nanotechnology 19 (2008) 215714.
[65] A. Burlacu, V.V. Ursaki, D. Lincot, V.A. Skuratov, T. Pauporte, E. Rusu, I.M. Tiginyanu, Enhanced radiation hardness of ZnO nanorods versus bulk layers, Phys. Status Solidi-rapid Res. Lett. 2 (2008) 68–70.
[66] R.E. Peale, E.S. Flitsiyan, C. Swartz, O. Lupan, L. Chernyak, L. Chow, W.G. Vernetson, Z. Dashevsky, Neutron transmutation doping and radiation hardness for solution-grown bulk and nano-structured ZnO, Performance and Reliability of Semiconductor Devices, in: M. Mastro, J. LaRoche, F. Ren, J.-I. Chyi, J. Kim (Eds.). Mater. Res. Soc. Symp. Proc. Volume 1108, Warrendale, PA (2009) *Materials Research Society Symposium Proceedings* 1108, (2009) pp. 55-60.
[67] D.C. Look, D.C. Reynolds, J.W. Hemsky, R.L. Jones, J.R. Sizelove, Production and annealing of electron irradiation damage in ZnO, Appl. Phys. Lett. 75 (1999) 811–813.
[68] F.D. Auret, S.A. Goodman, M. Hayes, M.J. Legodi, H.A. van Laarhoven, D.C. Look, Electrical characterization of 1.8 MeV proton-bombarded ZnO, Appl. Phys. Lett. 79 (2001) 3074–3076.
[69] S.O. Kucheyev, C. Jagadish, J.S. Williams, P.N.K. Deenapanray, M. Yano, K. Koike, S. Sasa, M. Inoue, K. Ogata, Implant isolation of ZnO, J. Appl. Phys. 93 (2003) 2972–2976.
[70] D. Weisenberg, M. Dürrschnabel, D. Gerthsen, F. Pérez-Willard, A. Reiser, G.M. Prinz, M. Feneberg, K. Thonke, R. Sauer, Conductivity of single ZnO nanorods after Ga implantation in a focused-ion-beam system, Appl. Phys. Lett. 91 (2007) 132110.
[71] R. Ferro, J.A. Podriguez, P. Bertrand, Development and characterization of a sprayed ZnO thin film-based NO_2 sensor, Phys. Status Solidi (c) 2 (2005) 3754–3757.
[72] H.-M. Lin, S.-J. Tzeng, P.-J. Hsiau, W.-L. Tsai, Electrode effects on gas sensing properties of nanocrystalline zinc oxide, Nanostruct. Mater. 10 (1998) 465–477.
[73] J.X. Wang, X.W. Sun, Y. Yang, H. Huang, Y.C. Lee, O.K. Tan, L. Vayssieres, Hydrothermally grown oriented ZnO nanorod arrays for gas sensing applications, Nanotechnology 17 (2006) 4995–4998.
[74] N. Barsan, U. Weimar, Conduction model of metal oxide gas sensors, J. Electroceram. 7 (2001) 143–167.
[75] A. Heilig, N. Bârsan, U. Weimar, M. Schweizer-Berberich, J.W. Gardner, W. Göpel, Gas identification by modulating temperatures of SnO_2-based thick film sensors, Sens. Actuators B: Chem. 43 (1997) 45–51.
[76] H. Nanto, T. Minami, S. Takata, Zinc-oxide thin-film ammonia gas sensors with high sensitivity and excellent selectivity, J. Appl. Phys. 60 (1986) 482–484.
[77] V. Demarne, S. Balkanova, A. Grisel, D. Rosenfeld, F. Lévy, Integrated gas sensor for oxygen detection, Sens. Actuators B: Chem. 19 (1994) 497–498.
[78] P. Qi, O. Vermesh, M. Grecu, A. Javey, Q. Wang, Hongjie Dai, S. Peng, K.J. Cho, Toward large arrays of multiplex functionalized carbon nanotube sensors for highly sensitive and selective molecular detection, Nano Lett. 3 (2003) 347–351.
[79] Y. Zhang, A. Kolmakov, S. Chretien, H. Metiu, M. Moskovits, Control of catalytic reactions at the surface of a metal oxide nanowire by manipulating electron density inside it, Nano Lett. 4 (2004) 403–407.
[80] J. Riu, A. Maroto, F.X. Rius, Nanosensors in environmental analysis, Talanta 69 (2006) 288–301.
[81] S. Saito, M. Miyayama, K. Kuomoto, H. Yanagida, Gas sensing characteristics of porous ZnO and Pt/ZnO ceramics, J. Am. Ceram. Soc. 68 (1985) 40–43.
[82] D. Kohl, The role of noble metals in the chemistry of solid-state gas sensors, Sens. Actuators B: Chem. 1 (1990) 158–165.
[83] J.B.K. Law, J.T.L. Thang, Improving the NH_3 gas sensitivity of ZnO nanowire sensors by reducing the carrier concentration, Nanotechnology 19 (2008) 205502.
[84] S.R. Morrison, Semiconductor gas sensors, Sens. Actuators 2 (1981) 329–341.
[85] IEEE Trans. Nanotechnol. 7 (6) (2008) 668–682.
[86] S. Basu, A. Dutta, Room-temperature hydrogen sensors based on ZnO, Mater. Chem. Phys. 47 (1997) 93–96.
[87] C. Soci, A. Zhang, B. Xiang, S.A. Dayeh, D.P.R. Aplin, J. Park, X.Y. Bao, Y.H. Lo, D. Wang, ZnO nanowire UV photodetectors with high internal gain, Nano Lett. 7 (2007) 1003–1009.
[88] D.H. Zhang, Adsorption and photodesorption of oxygen on the surface and crystallite interfaces of sputtered ZnO films, Mater. Chem. Phys. 45 (1996) 248–252.
[89] Q.H. Li, T. Gao, Y.G. Wang, T.H. Wang, Adsorption and desorption of oxygen probed from ZnO nanowire films by photocurrent measurements, Appl. Phys. Lett. 86 (2005) 123117–123119.
[90] K. Vanheusden, W.L. Warren, C.H. Seager, D.R. Tallant, J.A. Voigt, B.E. Gnade, Mechanisms behind green photoluminescence in ZnO phosphor powders, J. Appl. Phys. 79 (1996) 7983–7990.

Please cite this article in press as: O. Lupan, et al., Selective hydrogen gas nanosensor using individual ZnO nanowire with fast response at room temperature, Sens. Actuators B: Chem. (2009), doi:10.1016/j.snb.2009.10.038

[91] F.A. Kröger, Point defect in solids: physics, chemistry, and thermodynamics, in: R.N. Schock (Ed.), Point Defects in Minerals, American Geophysical Union, Washington, 1985, pp. 1–17.
[92] W. An, X. Wu, X.C. Zeng, Adsorption of O_2, H_2, CO, NH_3, and NO_2 on ZnO Nanotube: a density functional theory study, J. Phys. Chem. C 112 (2008) 5747–5755.
[93] R.P Eischens, W.A. Pliskin, M.J.D. Low, The infrared spectrum of hydrogen chemisorbed on zinc oxide, J. Catal. 1 (1962) 180–191.
[94] C. Wang, G. Zhou, J. Li, B. Yan, W. Duan, Hydrogen-induced metallization of zinc oxide $(2\bar{1}\bar{1}0)$ surface and nanowires: the effect of curvature, Phys. Rev. B 77 (2008) 245303.
[95] R.J. Kokes, Acc. Chem. Res. 6 (226) (1973) (references therein);
Z.L. Wang, Oxide nanobelts and nanowires—growth, properties and applications, J. Nanosci. Nanotechnol. 8 (2008) 27–55.

Biographies

O. Lupan received his MS in microelectronics and semiconductor devices from the Technical University of Moldova (TUM) in 1993. He received his PhD in solid state electronics, microelectronics and nanoelectronics from the Institute of Applied Physics, Academy of Sciences of Republic of Moldova in 2005. He is an Associate Professor (from 2008) and researcher scientist (from 1994) in solid state electronics, microelectronics and nanoelectronics at the Department of Microelectronics and Semiconductor Devices of the TUM. His current research interests range over semiconducting oxides micro-nano-architectures and thin films for chemical sensors, optoelectronic devices and solar cells; nanotechnologies with self-assembly, chemical and electrochemical depositions; development and investigation of novel micro-nano-devices.

V.V. Ursaki received his MS degree from the Moscow Institute of Physics and Engineering in 1979. He received his PhD degree in Semiconductor Physics from Lebedev Institute of Physics, Academy of Sciences of U.S.S.R., in 1986, and his Doctor habilitate degree in 1998 from the Institute of Applied Physics of the Academy of Sciences of Moldova. From 1986 he works at the Institute of Applied Physics of the Academy of Sciences of Moldova. His research interests are in the field of optical properties of semiconductor materials, lasing effects in solid state nanostructures, optoelectronic and photonic properties of nanostructures and nanocomposite materials. Email: ursaki@yahoo.com.

G. Chai is the Research Director at Apollo Technologies, Inc., Orlando, FL, USA. He received his B.S. in physics in 1999 from the Peking University, Beijing, China. He received Ph.D. in Condensed Matter Physics from University of Central Florida, Orlando, FL, USA in 2004. Research interest: ZnO nanorod sensors; Individual carbon nanotube devices, Focused Ion Beam fabrication of nanodevices. E-mail: guangyuchai@yahoo.com.

L. Chow is the associate chair and Professor of the Department of Physics University of Central Florida Orlando. He received his BS in physics in 1972 from the National Central University, Taiwan. He received PhD in Physics from Clark University, Worcester, MA, USA in 1981. In 1981–1982 was postdoc in physics at the University of North Carolina, Chapel Hill, NC. He joined University of Central Florida in 1983 as an assistant Professor, and was promoted to associate professor in 1988 and to professor in 1998. Areas of expertise: Chemical bath deposition, nanofabrications of carbon nanotubes and metal oxides, diffusion in semiconductors, high T_c thin film, hyperfine interactions, high pressure physics, thin films.

G.A. Emelchenko is the head of laboratory and Professor of the Institute of Solid State Physics RAS. He received his MS degree from the Ural Polytechnical Institute (Swerdlovsk, U.S.S.R.) in 1971. He received his PhD degree in Crystallography from the Institute of Crystallography of Russian Academy of Sciences in 1974, and his Doctor habilitate degree in 1992 from the Institute of Solid State Physics of Russian Academy of Sciences, Chernogolovka. His research interests are in the fields of synthesis, structure, phase equilibria, single crystal growth, nanoparticles and nanostructures fabrication, photonic crystals preparation and study of their optical properties. Email: emelch@issp.ac.ru

I.M. Tiginyanu received his PhD degree in Semiconductor Physics from Lebedev Institute of Physics, Moscow, in 1982. From 1984 to 1998 he worked as senior researcher at the Academy of Sciences of Moldova (ASM). In 2004 he was elected vice-president of the ASM. He serves as Director of the National Center for Materials Study and Testing. Professor Tiginyanu's research interests are related to nanotechnologies, photonic crystals, random lasing, cost-effective solar cells and new sensor technologies. He has 250 journal publications and 42 patents. He is member of AAAS, OSA, SPIE, MRS and Electrochemical Society. More information is available at http://www.ncmst.utm.md.

A.N. Gruzintsev received his MS degree from the Moscow Physical -Technical Institute in 1982. He received his PhD degree in Semiconductor Physics from the Moscow Physical -Technical Institute in 1985, and his Doctor habilitate degree in 1998 from the Ulaynovsk State University. From 1985 he works at the Institute of Microelectronics Technology and High Purity Materials, Russian Academy of Sciences. His research interests are in the field of optical properties of semiconductor materials, lasing effects in solid state nanostructures, optoelectronic and photonic properties of nanostructures and photonic crystals. Email: gran@iptm.ru.

A.N. Redkin received his MS degree from the Moscow State University in 1978. He received his PhD degree in Chemistry from the Moscow State University in 1985. From 1978 he works at the Institute of Microelectronics Technology and High Purity Materials, Russian Academy of Sciences. His research interests are in the field of chemistry of semiconductor materials, lasing effects in solid state nanostructures, optoelectronic and photonic properties of nanostructures. Email: arcadii@iptm.ru.

Please cite this article in press as: O. Lupan, et al., Selective hydrogen gas nanosensor using individual ZnO nanowire with fast response at room temperature, Sens. Actuators B: Chem. (2009), doi:10.1016/j.snb.2009.10.038